Operating range extension of cascaded H-bridge star using hybrid converter topology for STATCOM under unbalanced conditions

Ehsan Behrouzian, Massimo Bongiorno
CHALMERS UNIVERSITY OF TECHNOLOGY
Hörsalsvägen 11, SE-41296
Gothenburg, Sweden
Phone: +46317721655
Email: ehsan.behrouzian@chalmers.se
Email: massimo.bongiorno@chalmers.se

Jan R Svensson
ABB CORPORATE RESEARCH
Forskargränd 7, SE-72178
Västerås, Sweden
Phone: +4621324883
Email: jan.r.svensson@se.abb.com

Acknowledgments

The financial support provided by Energimyndigheten and ABB is gratefully acknowledged.

Keywords

≪Multilevel converters≫, ≪Converter control≫, ≪Static Synchronous Compensator (STATCOM)≫, ≪FACTS≫.

Abstract

A controller for a hybrid converter for STATCOM applications, based on a cascaded H-bridge star in series with a generic converter connected at the star point, is proposed. The controller utilizes the generic converter in an optimized way to maximize the operating range of the converter, with focus on unbalanced operating conditions. So for each operating condition, the generic converter reference voltage minimizes the voltage rating of the star part. Theoretical investigations of the hybrid converter using the proposed control approach show that the hybrid converter allows to effectively extend the operating range of the converter under unbalanced conditions of the system, given that the generic converter is large enough to circulate the needed active power between the converter phase legs. This indicates that, depending on the requirements from the operator in terms of negative-sequence injection capability, the hybrid converter can be a valuable solution to overcome the limitations of the CHB star.

Introduction

The market trend clearly indicates that Voltage Source Converter (VSC) based reactive-power compensator is more and more utilized in the power system, both for utility and industrial applications. When connected in shunt with the grid, the VSC system (also named STATic COMpensator, STATCOM) has a smaller footprint than the equivalent thyristor-based solution (or Static Var Compensator, SVC), a better dynamic performance and an increased robustness for weak-grid connection.

Among various VSC topologies, the Cascaded H-Bridge (CHB) star and delta are today the industrial standard for STATCOM applications [1], thanks to their modularity, simple scalability and lower converter rating requirements as compared with other topologies. The main disadvantage with the CHBs is the lack of a common DC link and thereby the difficulty in exchanging energy among the phase legs. The solution is to inject a properly controlled zero-sequence voltage in case of the CHB star [2, 3, 4, 5] or zero-sequence current in case of the CHB delta [6, 7, 8, 9]. However, the CHBs show a limited operating range under unbalanced system conditions, due to the presence of a singularity point and, thereby, the need for a high over-rating under certain circumstances [10].

Focusing on the CHB star, hybrid converters have been proposed as a solution to reduce the needed over-rating due to singularity [11]. The idea is to use the CHB star together with a Generic Converter (GC) connected to the converter's neutral point, in order to facilitate the energy exchange between the converter phases. Several works propose control techniques for the hybrid converter, mainly considering a 2-level converter as the GC. In [12, 13] the authors propose to generate a voltage component at the GC terminals having the same phase angle as the line current through a per-phase control, in order to generate a controlled active power that counteracts the power unbalance. Similar idea with active power support is suggested in [14]. However, in [14] the GC voltage amplitude is kept constant. Therefore, it is not possible to control the power exchanged between the phases. References [15, 16, 17] propose different control strategies for the GC to re-balance the capacitor voltages in the H-bridges. However, the main focus is on balanced system conditions. As an alternative, [18] suggests to use the zero-sequence voltage injection on the star part to facilitate the energy exchange while the GC partially generates the reference voltages. Each of these techniques utilizes the GC to generate only one specific type of voltage component. However, this might not lead to an effective GC utilization. More importantly, the impact of the hybrid converter utilization in extending the operating range of the STATCOM under unbalanced conditions as compared with the classical CHB star has not been addressed.

The aim of this paper is to propose propose a control algorithm for the hybrid converter to obtain an optimal utilization of the GC for STATCOM application and thus, minimizing the effect of the singularity point in the CHB star. The operating range of the hybrid converter is compared with the classical CHB star. The obtained results demonstrate that the operating range of the hybrid converter can be significantly improved, given that the GC is sufficiently large to circulate the needed energy between the converter phase-legs.

Hybrid converter topology

The investigated hybrid converter topology is illustrated in Fig. 1. The system consists of two parts. The CHB star (here denoted as "star part" in the figure) and the GC (displayed inside the dashed rectangle), connected to the neutral point of the star part. No specific topology is considered for the GC. However, it can generate any kind of reference voltages and exchange energy among its phases under any kind of unbalanced scenario[1]. Therefore, the GC in Fig. 1 is represented by three controllable AC voltage sources. The hybrid converter is connected to the grid via a filter reactor in each phase. The grid is modeled by a three-phase AC source with series reactors, representing the short-circuit impedance at the connection point. The steady-state operating principle is provided in this section using phasor analysis.

Operating principle

From the demanded positive- and negative-sequence current phasors($\underline{I}^+$,$\underline{I}^-$)[2], the converter reference voltages in steady-state are calculated as

$$\underline{V}^+ = \underline{E}^+ - (R_\mathrm{f} + j\omega L_\mathrm{f})\underline{I}^+, \qquad \underline{V}^- = \underline{E}^- - (R_\mathrm{f} - j\omega L_\mathrm{f})\underline{I}^- \tag{1}$$

where $\underline{E}^\pm$ are the Point of Common Coupling (PCC) positive- and negative-sequence voltage phasors, R_f and L_f are the filter resistance and inductance and finally ω is the line angular frequency.

In order to guarantee a stable operation of the hybrid converter, the capacitor voltages at the star part must be kept constant and equal to their reference value. For a lossless converter (100% efficiency), the capacitor voltages can be kept constant by controlling the average active power flowing in each phase of the star part to zero. This is naturally achieved under balanced conditions ($\underline{E}^- = \underline{I}^- = 0$) and when the STATCOM only exchanges reactive power with the grid. Fig. 2 (a) illustrates an example of the reference

[1] This assumption is made in order to allow the theoretical investigation to find the maximum possible improvement with the hybrid converter. The idea is to provide a comprehensive theoretical investigation with a generic converter rather than focusing on one specific GC topology. The reader should observe that the proposed control approach can be adopted to any specific selected topology for the GC.

[2] Phasor quantities are denoted by underlined capital letters, capital letters indicate the amplitude of the phasor and small letters show the AC instantaneous terms.

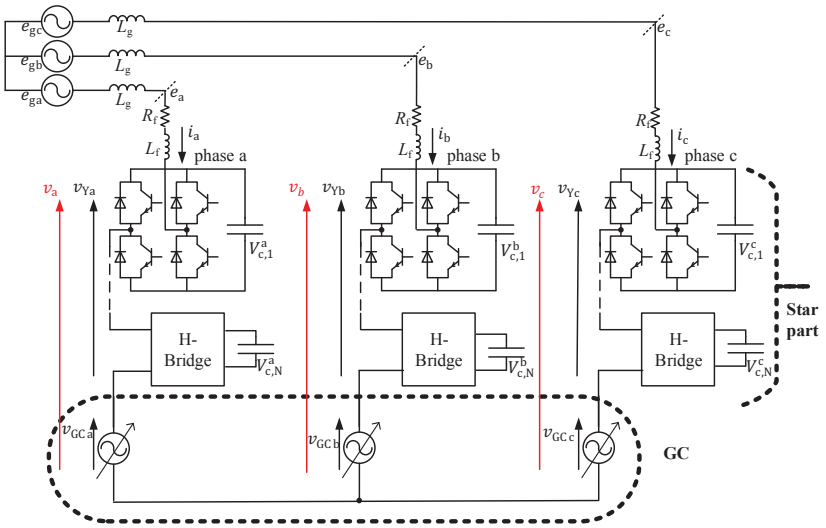

Fig. 1: Hybrid converter topology consisting of CHB star together with GC at the star point

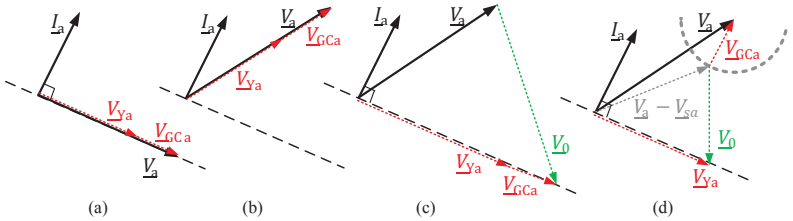

Fig. 2: Current and voltage phasors in phase *a*. (a) balanced condition, (b) unbalanced condition with non-zero average active power on the star part, (c,d) unbalanced condition with two possible voltage sharing to nullify the active power on the star part

voltage phasor ($\underline{V}_\mathrm{a}$) and line current ($\underline{I}_\mathrm{a}$) in phase-*a* under a balanced condition. $\underline{V}_\mathrm{a}$ is perpendicular to $\underline{I}_\mathrm{a}$, result in zero average active power. For this example, $\underline{V}_\mathrm{a}$ is shared between the star part ($\underline{V}_\mathrm{Ya}$) and the GC ($\underline{V}_\mathrm{GCa}$) as shown in the figure. $\underline{V}_\mathrm{Ya}$ and $\underline{V}_\mathrm{GCa}$ have the same phase angle as $\underline{V}_\mathrm{a}$.

For unbalanced conditions, the reference voltage phasor for each phase may not necessarily be perpendicular to its corresponding line current. Fig. 2 (b) illustrates $\underline{V}_\mathrm{a}$ and $\underline{I}_\mathrm{a}$ under a hypothetical unbalanced condition. Sharing $\underline{V}_\mathrm{a}$ in the same way as in the balanced case depicted in Fig. 2 (a) results in non-zero average active power in phase-*a* of the star part, which will cause the capacitor voltages in the phase leg to diverge from their reference value.

To nullify the active power during unbalanced conditions, a zero-sequence voltage ($\underline{V}_0$) is normally superimposed to the reference voltage. An example of such scenario is displayed in Fig. 2 (c). The resulting reference voltage ($\underline{V}_\mathrm{a} + \underline{V}_0$) can then be shared between the star part and the GC. Although this can be an approach to utilize the GC, several other possible voltage sharing can also be defined.

To further clarify the concept, Fig. 2 (d) shows another voltage sharing example. The arc that is shown with the gray dashed line is part of a circle having radius equal to the voltage rating of the GC. Any voltage phasor inside this circle can be a possible reference voltage for the GC. The resulting $\underline{V}_\mathrm{Ya}$ with the selected $\underline{V}_\mathrm{GCa}$ shown in Fig. 2 (d) may then be smaller than the previous case. When considering all the three phases and all the possible voltage combinations, there will be a set of three-phase voltages for the GC that leads to a minimum voltage rating for the star part. This set of three-phase voltages must then be selected for the GC.

Proposed algorithm

The basic principle behind the proposed algorithm is to identify all possible voltage phasors for the GC and select the one that results in the minimum voltage rating for the star part. Normally, in STATCOM

application the converter cannot exchange active power in steady state. This restriction must be considered in the selection of the voltage phasors of the GC. Therefore, solutions resulting in non-zero total active power in the GC are disregarded. The block diagram of the proposed control algorithm is shown in Fig. 3 (blue and white blocks) and is described step by step as follows. Note that in this paper the positive-sequence grid-voltage phasor is taken as the reference. Therefore, the quadratic component of the positive-sequence current ($I_{\mathrm{q}}^{+} = I^{+}\sin(\angle\overline{I}^{+})$) impacts only the positive-sequence reactive power, while its direct component ($I_{\mathrm{d}}^{+} = I^{+}\cos(\angle\overline{I}^{+})$) impacts only the positive-sequence active power. The negative-sequence current ($\underline{I}^{-}$) is normally perpendicular to the grid negative-sequence voltage in order to avoid negative-sequence active power exchange. Therefore, $\underline{I}^{-}$ is considered as the negative-sequence reactive current.

Following Fig. 3 from top, the maximum voltage rating of the GC ($V_{\mathrm{GC,max}}$) and the demanded reactive currents for each sequence ($\underline{I}^{-}$ and I_{q}^{+} for the negative- and positive-sequences respectively) are set first. For a lossless converter ($I_{\mathrm{d}}^{+} = 0$), $\underline{I}^{+}$ is calculated next. Having the demanded current phasors, the converter reference voltages are then calculated from (1). Using the symmetrical component basics, the three-phase reference voltage ($\underline{V}_{\mathrm{abc}}$) is calculated next.

At this point the algorithm starts searching between all possible voltage phasors for the GC to find the one that leads to the minimum voltage rating on the star part. For this purpose, a loop is activated where every possible phase angle and amplitude for each phase leg of the GC ($0 \leq \angle\underline{V}_{\mathrm{GC,abc}} < 2\pi$ and $0 \leq V_{\mathrm{GC,abc}} \leq V_{\mathrm{GC,max}}$) is considered. As mentioned earlier, the reference voltages for the GC that result in non-zero total average power must be disregarded. Therefore the total three-phase power caused by the selected reference voltages for the GC is calculated. If the power is not equal to zero, the considered $\underline{V}_{\mathrm{GC,abc}}$ is disregarded and the loop starts over. Otherwise, the loop continues with calculating the remaining part of the reference voltage ($\underline{V}_{\mathrm{r,abc}}$), which must be synthesized by the star part of the hybrid converter. However, $\underline{V}_{\mathrm{r,abc}}$ may not necessarily result in zero average-power in each phase leg of the star part. Therefore, a zero-sequence voltage must be superposed to $\underline{V}_{\mathrm{r,abc}}$. The required zero-sequence voltage ($\underline{V}_{0}$) is calculated in the same way as described in [10]:

$$V_0 = \frac{-k_1}{k_3\cos(\angle\underline{V}_0) + k_4\sin(\angle\underline{V}_0)}, \qquad \angle\underline{V}_0 = \mathrm{tg}^{-1}\left(\frac{k_2k_3 - k_1k_5}{k_1k_6 - k_2k_4}\right) \tag{2}$$

with

$$\begin{aligned}
k_1 &= \mathrm{Re}\{\underline{V}_{\mathrm{r}}^{+}\underline{I}^{-*}\} + \mathrm{Re}\{\underline{V}_{\mathrm{r}}^{-}\underline{I}^{+*}\} + \mathrm{Re}\{\underline{V}_{\mathrm{r}}^{0}\underline{I}^{-*}\} + \mathrm{Re}\{\underline{V}_{\mathrm{r}}^{0}\underline{I}^{+*}\} \\
k_2 &= \mathrm{Re}\{\underline{V}_{\mathrm{r}}^{+}\underline{I}^{-*}e^{-\mathrm{j}4\pi/3}\} + \mathrm{Re}\{\underline{V}_{\mathrm{r}}^{-}\underline{I}^{+*}e^{\mathrm{j}4\pi/3}\} + \mathrm{Re}\{\underline{V}_{\mathrm{r}}^{0}\underline{I}^{-*}e^{-\mathrm{j}2\pi/3}\} + \mathrm{Re}\{\underline{V}_{\mathrm{r}}^{0}\underline{I}^{+*}e^{+\mathrm{j}2\pi/3}\} \\
k_3 &= \mathrm{Re}\{\underline{I}^{+} + \underline{I}^{-}\}, k_4 = \mathrm{Im}\{\underline{I}^{+} + \underline{I}^{-}\} \\
k_5 &= \mathrm{Re}\{\underline{I}^{+}e^{-\mathrm{j}2\pi/3} + \underline{I}^{-}e^{\mathrm{j}2\pi/3}\}, k_6 = \mathrm{Im}\{\underline{I}^{+}e^{-\mathrm{j}2\pi/3} + \underline{I}^{-}e^{\mathrm{j}2\pi/3}\}
\end{aligned}$$

Thus, the three-phase voltage phasors for the star part ($\underline{V}_{\mathrm{Y,abc}}$) are calculated and the amplitude of the phase leg with the highest peak ($V_{\mathrm{Y,peak}}$) and the selected GC voltage phasors are saved. The loop starts over with a new set of three-phase voltage for the GC. When the loop ends, the minimum value of $V_{\mathrm{Y,peak}}$ among all the saved values shows the lowest possible voltage rating that can be obtained for the star part ($V_{\mathrm{Y,min}}$). The corresponding three-phase reference voltage phasor for the GC are then selected as the optimum reference voltages for the GC.

A special case is when the STATCOM is equipped with a temporary energy storage (e. g., super capacitors connected to the dc side of the GC), for example to facilitate the integration of renewable energy sources into the power systems. In such a case, the available active power can be utilized for balancing purposes and can be used to further minimize the voltage rating of the star part. Note that the resulting active power must be exchanged with the grid to keep the total power on the star part equal to zero. Taking the positive-sequence component of the grid voltage as a reference ($\underline{E}^{+} = E^{+}$) and assuming that the grid voltage is balanced ($\underline{E}^{-} = 0$), the active power flowing in the star part for a given $\underline{I}^{-}$ and I_{q}^{+} will

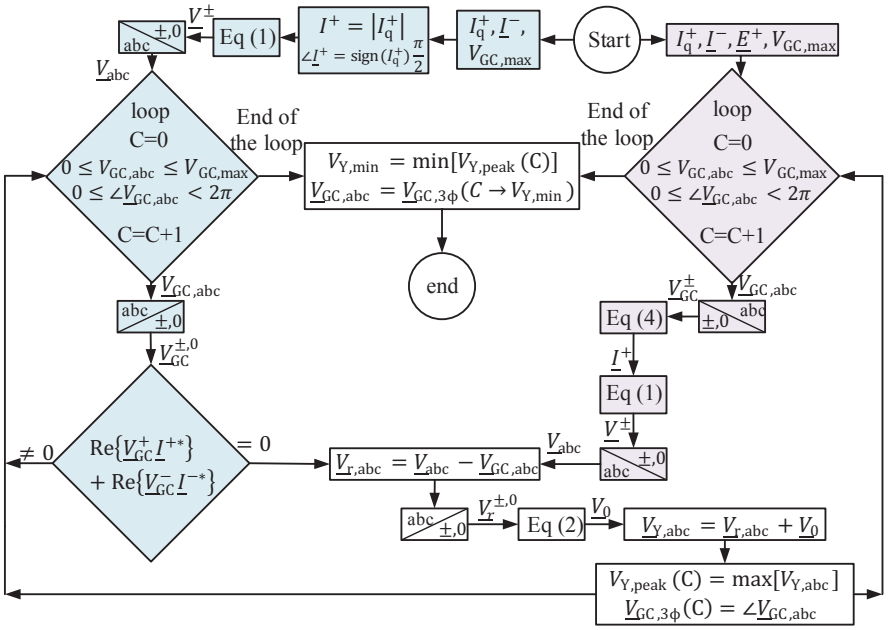

Fig. 3: Proposed algorithm for the hybrid converter, blue and white blocks: without energy storage at GC; Gray and white blocks: with energy storage at GC

remain zero if

$$\text{if} \quad I_q^+ \neq 0 \Rightarrow \text{Re}\left\{\underline{V}_{GC}^+ \underline{I}^{+*}\right\} + \text{Re}\left\{\underline{V}_{GC}^- \underline{I}^{-*}\right\} = E^+ \text{Re}\left\{\underline{I}^{+*}\right\} \quad , \quad I_q^+ = I^+ \sin(\angle \underline{I}^+)$$

$$\text{if} \quad I_q^+ = 0 \Rightarrow \begin{cases} \angle \underline{I}^+ = 0 \quad , \quad V_{GC}^+ I^+ \cos\left(\angle \underline{V}_{GC}^+\right) + \text{Re}\left\{\underline{V}_{GC}^- \underline{I}^{-*}\right\} = E^+ I^+ \\ \text{or} \\ \angle \underline{I}^+ = \pi \quad , \quad -V_{GC}^+ I^+ \cos\left(\angle \underline{V}_{GC}^+\right) + \text{Re}\left\{\underline{V}_{GC}^- \underline{I}^{-*}\right\} = -E^+ I^+ \end{cases} \tag{3}$$

$\underline{I}^+$ is then determined by fulfilling (3) as:

$$\text{if } I_q^+ \neq 0 \Rightarrow \angle \underline{I}^+ = \tan^{-1}\left[\frac{E^+ I_q^+ - V_{GC}^+ I_q^+ \cos\left(\angle \underline{V}_{GC}^+\right)}{V_{GC}^+ I_q^+ \sin\left(\angle \underline{V}_{GC}^+\right) + \text{Re}\left\{\underline{V}_{GC}^- \underline{I}^{-*}\right\}}\right] \quad , \quad I^+ = \frac{I_q^+}{\sin(\angle \underline{I}^+)}$$

$$\text{if } I_q^+ = 0 \Rightarrow I^+ = \left|\underbrace{\frac{-\text{Re}\left\{\underline{V}_{GC}^- \underline{I}^{-*}\right\}}{V_{GC}^+ \cos\left(\angle \underline{V}_{GC}^+\right) - E^+}}_{T}\right| \quad , \quad \angle \underline{I}^+ = \begin{cases} 0 & \text{if} \quad T > 0 \\ \pi & \text{if} \quad T < 0 \end{cases} \tag{4}$$

The resulting control strategy is shown in Fig. 3 (gray and white blocks). The algorithm starts by setting the maximum voltage rating of the GC, demanded $\underline{I}^-$ and I_q^+ and the grid voltage ($\underline{E}^+$). Similar to the case explained before, a loop starts afterward to evaluate every possible voltage phasor for the GC; as a difference compared with the previous strategy, voltage phasors that result in non-zero total power for the GC are also considered. For each voltage phasor, $\underline{I}^+$ is calculated from (4) for power balancing. Thus, the corresponding reference voltages are calculated. The remaining part of the algorithm is the same as for the previous case. At the end of the loop, the minimum value of $\underline{V}_{Y,peak}$ and the corresponding three-phase reference voltage phasor for the GC are selected.

Theoretical results

To evaluate the performance of the hybrid converter, several case studies are considered. In all cases, the grid voltage is balanced with amplitude of 1 pu ($\underline{E}^- = 0, \underline{E}^+ = 1$ pu). The positive-sequence reactive current (I_q^+) is set to 1 pu capacitive ($I_q^+ > 0$). This choice is dictated by the fact that capacitive mode im-

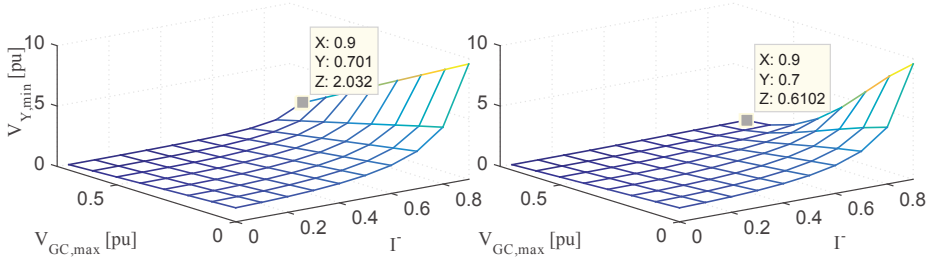

Fig. 4: Star part voltage rating versus GC voltage and negative-sequence current, on left without energy storage and on right with energy storage

poses higher voltage demands for the converter as compared with the inductive mode. The amplitude of the negative-sequence reactive current (I^-) varies from 0 to 0.9 pu. The negative-sequence current angle can be arbitrarily selected in the polar frame, depending on the requirements. However, as described in [10], the negative-sequence current angle that leads to the highest voltage demand for capacitive positive-sequence current is $\angle \underline{I}^- = {}^{\pi}/_{2}$; therefore, this angle is here considered for the negative-sequence current. Finally, a filter reactance and resistance of $X_f = 0.15$, $R_f = 0.015$ pu, with $\omega = 2\pi 50$ rad/s, are considered. It should be highlighted that the case with $I^- = 1$ pu (equal positive- and negative-sequence reactive currents) leads to the singularity point, resulting in an infinite zero-sequence voltage demand for the CHB star.

For each of the above mentioned cases, the voltage rating of the GC ($V_{GC,max}$) varies between 0 pu and 0.7 pu and for each value of $V_{GC,max}$ the algorithm displayed in Fig. 3 calculates the minimum voltage rating that can be obtained for the star part ($V_{Y,min}$). Fig. 4 shows $V_{Y,min}$ versus $V_{GC,max}$ and I^-. The plot on the left side displays the result without energy storage in the GC, while the plot on the right displays the result with energy storage. Starting with $V_{GC,max} = 0$ (equivalent to the classical CHB star), it can be observed that an increase in I^- leads to an increase in $V_{Y,min}$; high voltage requirements are obtained when the negative-sequence current approaches 1 pu (singularity point). Assuming for example that the rated voltage for the star part is 2 pu ($V_{Y,min}$ =2) and that $V_{GC,max} = 0$, the operating range is limited to $I^- < 0.6$ pu for the considered case study. With $V_{Y,min}$ =3 pu the operating range can be extended to $I^- < 0.7$ pu.

Focusing now on the left side figure (no energy storage) and assuming $V_{Y,min}$ =2 pu and $V_{GC,max} = 0.7$, the operating range can be extended to $I^- < 0.9$ pu. This means that by a total voltage rating of $V_{tot} = V_{Y,min} + V_{GC,max} = 2.7$ pu, the operating range can be effectively improved as compared with the classical CHB star. Further investigation has shown that with $V_{GC,max}$=1 pu, any kind of unbalanced condition can be covered. The results on the right side (GC with energy storage) shows additional improvements in the operating range of the hybrid converter, as the same operating range considered in the previous case ($I^- < 0.9$ pu) can now be obtained with $V_{Y,min}$ =2 pu and $V_{GC,max} = 0.4$ (V_{tot}=2.4 pu).

To further demonstrate the effectiveness of the hybrid converter, Fig. 5 (top plots) shows the trend of $V_{Y,min}$ versus $V_{GC,max}$ for $I^- = [0, 0.5, 0.9]$ pu and $I_q^+ = 1$ pu. The bottom plots show the total converter voltage $V_{tot} = V_{Y,min} + V_{GC,max}$ versus $V_{GC,max}$ for the same cases. Blue and red colors show the results for a system without and with energy storage, respectively. The obtained results show that using GC, not only lower voltage ratings will be required for the star part, the overall voltage rating of the converter is also reduced as compared with the classical CHB star (equivalent to $V_{GC,max} = 0$). It can also be observed that the GC with energy storage is more effective in reducing the voltage requirement than the GC without energy storage. It should be highlighted that not only the singularity point, but also those operating conditions close to the singularity point, for example $I^- = 0.9$ pu, are practically not feasible to be covered by the CHB star due to the extremely high voltage requirements. On the other hand, the hybrid converter can effectively extend the operating range of the CHB star with a drastic reduction in the total voltage requirement.

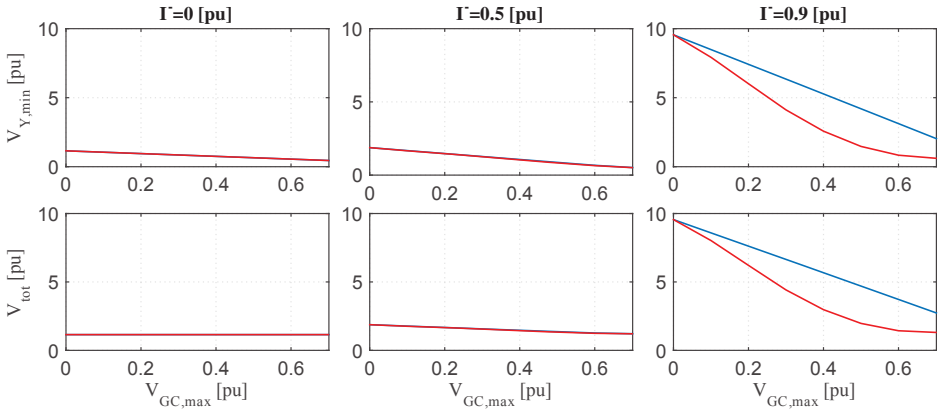

Fig. 5: Top plots: star part voltage rating versus GC voltage and bottom plots: total voltage versus GC voltage for $I^- = 0, 0.5, 0.9$ pu and $I_q^+ = 1$ pu, blue: without and red: with energy storage

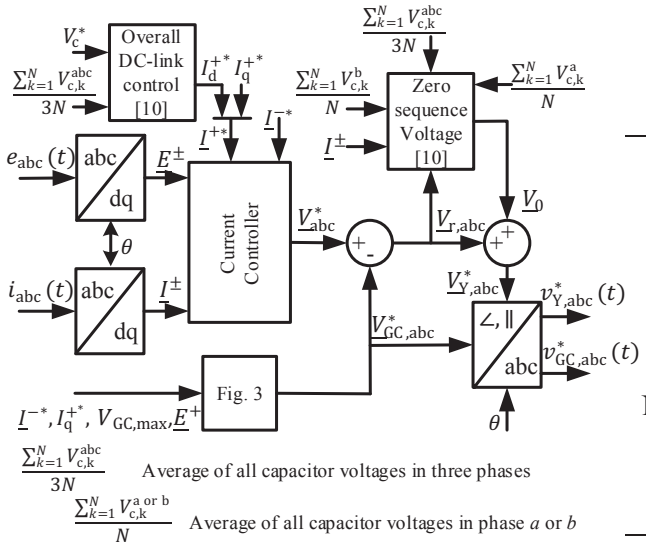

Fig. 6: Control block diagram of hybrid converter

Table I: System parameters in Fig. 1

Rated power	S	120 MVA
Grid peak voltage	E_g	27 kV
Grid inductance	L_g	0 H
Filter inductance	L_f	4.3 mH
Filter resistor	R_f	0.136 Ω
Cell capacitor size	C	4mF
Cell capacitor voltage	V_c^*	27 kV
Number of cells per phase	N	3
Grid frequency	f_o	50 Hz
Sampling frequency	f_s	6 kHz
Cell switching frequency	f_{sw}	2 kHz

Control implementation and simulation results

In this section, the control implementation and simulation results are presented. Fig. 6 shows the control block diagram for the hybrid converter in Fig. 1. The PCC voltages and line currents are measured and transferred to the $dq-$frame using the transformation angle (θ), which is typically determined by the Phase-Locked Loop (PLL) (not shown in the figure for clarity). The positive- and negative-sequence reference reactive currents $\underline{I}^{-*}, I_q^{+*}$ are set to the desired value, while I_d^{+*} is used to control the overall capacitor voltages to the reference value V_c^*. Next, the current controller determines the reference voltage of each phase ($\underline{V}^*_{abc}$). The reference voltages for the GC ($\underline{V}^*_{GC,abc}$) are calculated through the algorithm described in Fig. 3. The remaining part of the reference voltages ($\underline{V}_{r,abc}$) are determined by subtracting $\underline{V}^*_{abc}$ and $\underline{V}^*_{GC,abc}$. The required zero-sequence voltage needed to nullify the active power in each phase-leg of the star part is then calculated and superposed to the remaining part of the reference voltages, to obtain the reference voltages for the star part ($\underline{V}^*_{Y,abc}$). More information about the overall DC-link control and zero-sequence voltage calculation is found in [10]. The reference voltages in time domain for the star part ($v^*_{Y,abc}(t)$) and the GC ($v^*_{GC,abc}(t)$) are finally calculated. The modulators generate the switching pulses for the converters to synthesize the reference voltages for each stage.

The modulation technique for the star part is based on cell sorting approach. At each control cycle, assuming the state of the phase leg is in the charging mode (current direction toward converter and ref-

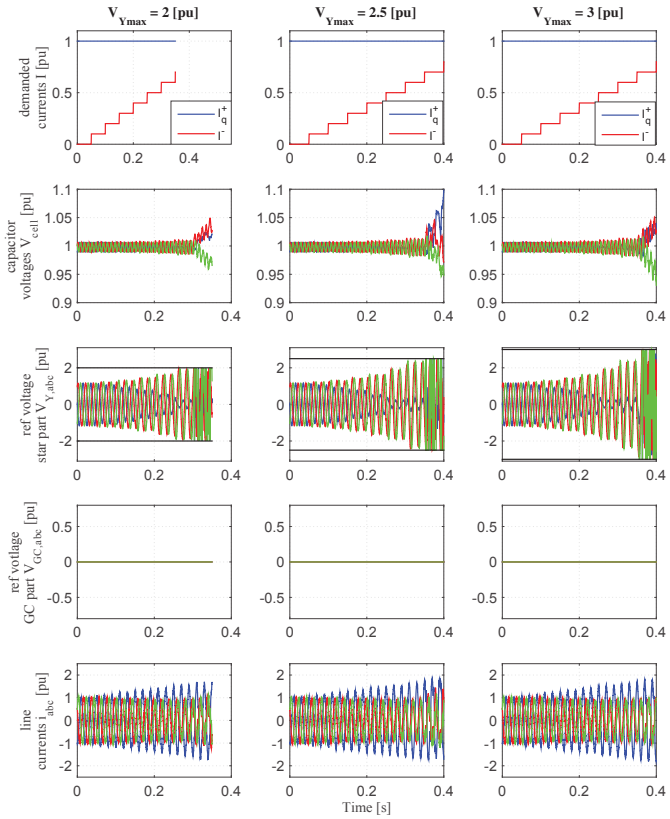

Fig. 7: Simulation results of hybrid converter without GC, results from top are: I_{q}^{+} and I^{-}, capacitor voltages, reference voltage of star, reference voltage of GC and line current

erence voltage and current at each phase have the same sign), the capacitors at each phase are sorted in ascending order. The reference voltage is, thus, modulated using capacitors with the lowest voltage. The same process is used for discharging mode (voltage and current at each phase are in opposite sign). However, at the discharging mode the capacitors with highest voltages are used instead. For The reference voltages for the GC can be directly used for the controllable AC sources.

Simulation results

The hybrid converter in Fig. 1 is simulated in PSCAD using the control algorithm in Fig. 6. Table I provides the system parameters used for the simulations.

The first simulation is conducted for the hybrid converter without the GC, i.e., the classical CHB star and the obtained results are shown in Fig. 7. The per-unit I_{q}^{+} and I^{-} are shown on the top plots. Per-unit capacitor voltages (V_{cell}), three-phase reference voltage for the star part and GC ($V_{\mathrm{Y,abc}}$ and $V_{\mathrm{GC,abc}}$, respectively) and three-phase line current (i_{abc}) are shown respectively from top after the demanded currents.

The I_{q}^{+} is set to 1 pu for the entire simulation time while I^{-} is set to zero at t=0 s and then increased in steps of 0.1 pu after each 0.05 s. Three voltage ratings of 2, 2.5 and 3 pu are considered for the CHB star. Starting with the 2 pu voltage limit for the CHB star, it can be observed that by increasing the negative-sequence current, the reference voltages for the CHB star are increased until they hit the limit of 2 pu at t=0.3 s, which corresponds to I^{-}=0.6 pu. A hard limiter limits the voltage references to avoid over modulation. Consequently, higher negative-sequence current demand will lead to diverging capacitor voltages. With 2.5 and 3 pu voltage ratings for the CHB star, the operating range of the converter is extended up to I^{-}=0.7 pu. The simulation results are well matched with the obtained theoretical results.

The second simulation performed considers the hybrid converter including the GC with no active-power exchange capability. The same operating conditions as for the previous case study are considered. The

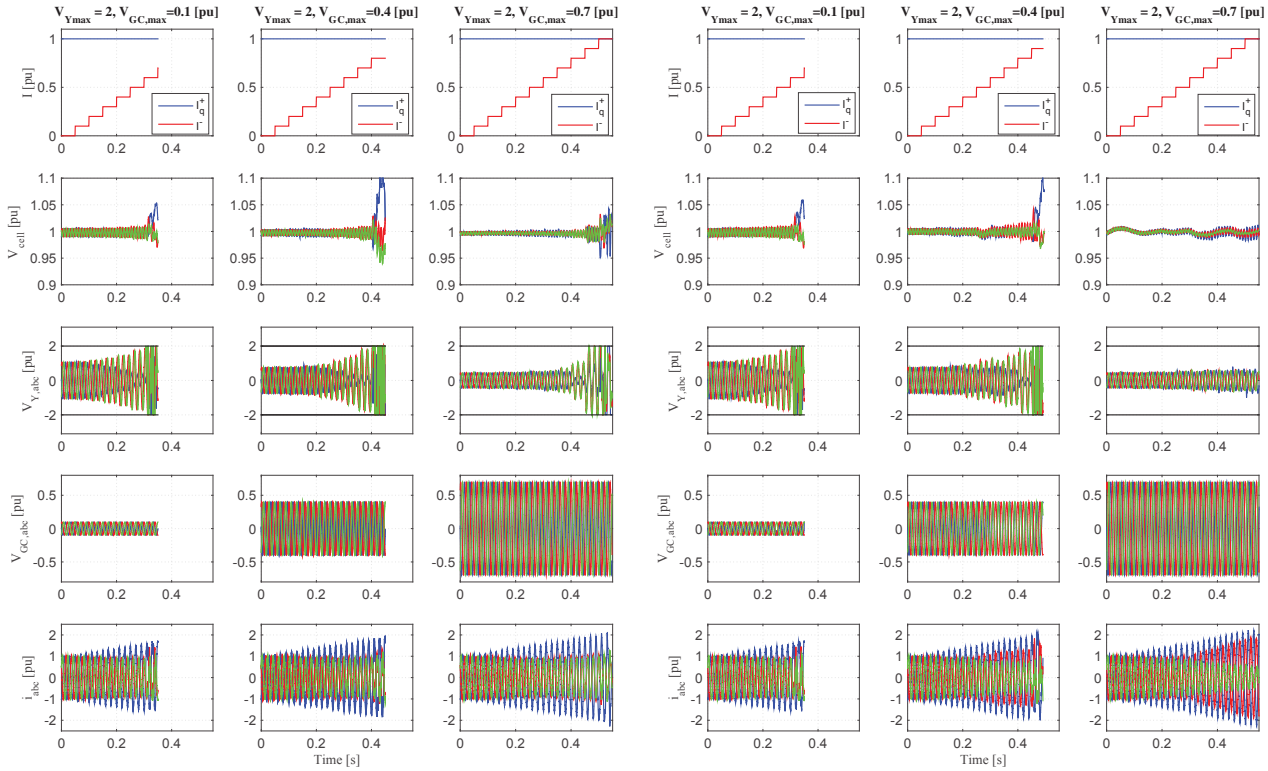

(a) without active power exchange

(b) with active power exchange

Fig. 8: Simulation results of hybrid converter without and with active power exchange capability in (a) and (b) respectively, priority of results are same as in Fig. 7

maximum voltage rating of the star part (V_{Ymax}) is set to 2 pu. Three voltage ratings for the GC are considered ($V_{\text{GC,max}} = 0.1$, 0.4 and 0.7 pu) and the obtained results are shown in Fig. 8 (a).

Starting with $V_{\text{Ymax}} = 2$ and $V_{\text{GC,max}} = 0.1$ pu and then increase the negative-sequence current, $V_{\text{Y,abc}}$ increases until the limit of 2 pu is reached at t=0.3 s, which corresponds to I^{-}=0.6 pu. This proves low-voltage rating for the GC does not allow to extend the operating range as compared with the classical CHB star. However, setting $V_{\text{GC,max}}$ to 0.4 and 0.7 pu allows the hybrid converter to properly operate up to I^{-}=0.8 pu and I^{-}=0.9 pu, respectively. Note that, as observed before, the CHB star can operate up to I^{-}=0.7 pu even with the 3 pu voltage rating. These simulations again validate the obtained theoretical results.

The same case study has been considered when assuming that the CB is equipped with a temporary energy storage and the results are displayed in Fig. 8 (b). Note that operation up to I^{-}=1 pu for $V_{\text{GC,max}} = 0.7$ pu can be achieved.

From the obtained results it can be concluded that the use of a hybrid converter effectively allows to extended the operating range of the CHB start when operated under unbalanced conditions. However, it is important to stress that the operating range extension is tightly dependent on the GC's ratings.

Conclusion

A controller for a hybrid converter for STATCOM applications, based on a Cascaded H-Bridge (CHB) star in series with a generic converter installed at its star point, is here proposed and investigated. For a given three-phase reference voltage, the reference voltage for the generic converter is calculated aiming at minimizing the reference voltage of the star part. Thus, the maximum possible operating range for unbalanced currents is achieved. Both cases with and without active power exchange capabilities for the converter are considered in the proposed controller. Theoretical investigation of the hybrid converter using the proposed control approach shows that the operating range of the STATCOM can be significantly

extended as compared with the classical CHB star. Temporary active power exchange capability can further extend the operating range. The resulting operating range for the hybrid converter is tightly linked to the ratings of the generic converter, which needs to be sufficiently large to be able to circulate the needed active power between the converter's phase legs. This indicates that, depending on the requirements from the operator in terms of negative-sequence injection capability, the hybrid converter can be a valuable solution to overcome the limitations of the CHB star.

References

[1] Sood V.K.: HVDC and FACTS Controllers - Applications of Static Converters in Power Systems, Boston: Kluwer Academic Publishers, 2004

[2] Yutaka Ota J.I., Shibano Y., Akagi H.: A Phase-Shifted PWM D-STATCOM Using a Modular Multilevel Cascade Converter (SSBC); Part II: Zero-Voltage-Ride-Through Capability, IEEE Trans. on Ind. Appl. 2015 Vol 51 no 1, pp. 289- 296

[3] Song Q., Liu W.: Control of a Cascade STATCOM With Star Configuration Under Unbalanced Conditions, IEEE Trans. on Power Electro. 2009 Vol 24 no 1, pp. 45- 58

[4] Hatano N., Ise T.: Control Scheme of Cascaded H-Bridge STATCOM Using Zero-Sequence Voltage and Negative-Sequence Current, IEEE Trans. on Power Del. 2010 Vol 25 no 2, pp. 543- 550

[5] Tan L., Wang S., Wang P., Li Y., Ge Q., Ren H., Song p.: High performance controller with effective voltage balance regulation for a cascade STATCOM with star configuration under unbalanced conditions, Proc. of 15th European Conference on Power Electronics and Applications (EPE) 2013

[6] Nieves M., Maza J.M., Mauricio J.M., Teodorescu R., Bongiorno M., Rodriguez P.: Enhanced control strategy for MMC-based STATCOM for unbalanced load compensation, Proc. of Power Electronics and Applications (EPE'14-ECCE Europe), 2014

[7] Hagiwara M., Maeda R., Akagi H.: Negative-Sequence Reactive-Power Control by a PWM STATCOM Based on a Modular Multilevel Cascade Converter (MMCC-SDBC), IEEE Trans. on Ind. Appl. 2012 Vol 48 no 2, pp. 720- 729

[8] Betz R.E., Summers T., Furney T.: Symmetry Compensation using a H-Bridge Multilevel STATCOM with Zero Sequence Injection, Proc. of 41st Industry Applications Conference (IAS). 2006 Vol 4, pp. 1724- 1731

[9] Du S., Liu J., Lin J., He Y.: Control strategy study of STATCOM based on cascaded PWM H-bridge converter with delta configuration, Proc. of 7th International Power Electronics and Motion Control Conference (IPEMC). 2012 Vol 1, pp. 345- 350

[10] Behrouzian E., Bongiorno M.: Investigation of Negative-Sequence Injection Capability of Cascaded H-Bridge Converters in Star and Delta Configuration, IEEE Trans. on Power Electro. 2017 Vol 32 no 2, pp. 1675- 1683

[11] Dijkhuizen F., Nami A., Zelaya H., Townsend C.D., (2014): A converter arrangment for power compensation and a method for controlling a power converter.. WO2014/194968A1.

[12] Townsend C.D., Tormo D., De-La-Parra H.Z.: One dimensional cell inversion: A modulation strategy for hybrid cascaded converters, IEEE Energy Conversion Congress and Exposition (ECCE), pp. 4653- 4660, 2014

[13] Zhang M., Li J., Chi B., Wang Q., Li G., Ye Q.: A novel generalized multilevel converter with the application in D-STATCOM, 12th IEEE Conference on Industrial Electronics and Applications (ICIEA), pp. 871- 875, 2017

[14] Chen Q., Gao N., Li R., Cai X., Lu Z.: A Novel STATCOM with limited active power support based on hybrid cascaded multilevel converter, International Power Electronics and Application Conference and Exposition, 2015

[15] Yang R., Zhang Y., Li B., Xu R., Yu Y., Xu D.: A new cascaded multilevel converter topology with energy exchange unit for STATCOM application, 2015 9th International Conference on Power Electronics and ECCE Asia (ICPE-ECCE Asia), pp. 2758- 2763, 2015

[16] Yin R., Hu P., Jiang D., Liang Y., Du Y., Lin Z.: Analysis of Hybrid Cascaded Multilevel Converter based STATCOM, IEEE 10th Conference on Industrial Electronics and Applications (ICIEA), pp. 643- 648, 2015

[17] Ziaeinejad S., Sangsefidi Y., Mehrizi-Sani A.: A Generalized Switching Strategy and Capacitor Sizing Algorithm for Granular Multilevel Converters, IEEE Trans. on Ind. Electro. 2018 Vol 65 no 6, pp. 4443- 4453

[18] Su Y.C., Wu P.H., Cheng P.T.: Control of the hybrid cascaded converter under unbalanced conditions, IEEE Energy Conversion Congress and Exposition (ECCE), pp. 2858- 2565, 2017